Structure determination of silicene nanoribbons on Ag(110)

P. Espeter[1,2,4], C. Keutner[1,2], N.F. Kleimeier[3], P. Roese[1,2], K. Shamout[1,2], G. Wenzel[3], U. Berges[1,2], H. Zacharias[3], C. Westphal[1,2]

[1] Experimentelle Physik 1 - Technische Universität Dortmund, 44221 Dortmund, Germany
[2] DELTA - Technische Universität Dortmund, 44221 Dortmund, Germany
[3] Fakultät Physik - WWU Münster, 48149 Münster, Germany
[4]corresponding author: philipp.espeter@tu-dortmund.de

ABSTRACT

Since the discovery of graphene much effort has been put into the development of comparable two dimensional graphene analoga to the carbon group. Silicene is probably the most famous representative of these graphene analoga. Different silicene allotropes exist depending on the growth conditions, e.g. the substrate temperature during growth and the substrate itself. In this study we report on the successful preparation of silicene nano-ribbons on Ag(110) substrate and we address the question of the interaction between the substrate and the absorbed silicene nano-ribbons. We utilize low energy electron diffraction (LEED) and photoelectron spectroscopy (XPS) techniques for verifying growth of the nano-ribbons and analyzing substrate-absorbate interaction due to their high surface sensitivity.

Keywords: silicene, nano-ribbon, structure, LEED, XPS

1 INTRODUCTION

During the last years much interest arose in two-dimensional materials that are formed by elements from the same main group of the periodic system than carbon. The probably most famous representative is silicon with its allotrope called silicene nano-ribbons. These nano-ribbons typically grow on Ag(110) substrates along the $[\bar{1}10]$ direction and have a (5×2) periodicity with respect to the substrate [1]. Many approaches of determining the precise atom positions inside the unit cell resulted in a multiplicity of proposed structure models. The range of proposed structure models is from rectangular over pentagonal to hexagonal and from planar over buckeld to stacked [2-13]. We performed LEED- and XPS-measurements for proving a successful preparation of silicene nano-ribbons on Ag(110). Furthermore, we utilize XPS measurements for deducing a line of arguments that can be used for evaluating the proposed structure models. We will apply this line of arguments for evaluating the most recent proposed structure model, the so-called pentamer structure [6, 13].

2 EXPERIMENT

The sample preparation and XPS measurements were performed in an ultra-high vacuum chamber located at Beamlime 11 at the *Dortmunder Elektronen Speicherring Anlage* DELTA. The chamber is equipped with a 5-axes manipulator which allows moving the sample in x, y, and z direction as well as rotations of the azimuthal angle φ and the polar angle Θ. Also, the sample holder is equipped with an integrated heating stage. For sample preparation a sputter-gun and a direct-current silicon evaporator are mounted at the chamber. For XPS measurements a hemispherical electron analyser is available.
Preparation of the Ag(110) sample was performed by several cycles of sputtering and annealing with $E_{beam} = 600\,\mathrm{eV}$ and $T_{anneal} = 400\,^{\circ}\mathrm{C}$. It turned out that sputtering of the Ag(110) sample under an incident angle $45\,^{\circ}$ resulted in a foggy surface. This behaviour of the sample was preserved even if sputtered with Neon instead of Argon. Also, reduction of the Ar^+-ion energy down to 500 eV did not suppress the foggy haze at the surface. Only an increase of the sputtering angle to $70\,^{\circ}$ yielded a perfect Ag(110) surface. A LEED pattern of the (1x1)-reconstructed Ag(110) surface is shown in figure 1.

The XPS-spectrum of figure 2 shows the chemical composition of the sample. It is obvious that there are solely core-level peaks from pure silver, in particular Ag 4s at a kinetic energy of $E_{kin} = 560\,\mathrm{eV}$, Ag 4p at 590 eV, and Ag 3d at 280 eV. Due to their small cross-sections the Ag 4p and Ag 4s signals are much smaller than the prominent Ag 3d signal.
The Ag Auger-signals at kinetic energies of $E_{kin} = 275\,\mathrm{eV}$, 300 eV, 355 eV, and 340 eV correspond to the $M_{45}N_1N$, $M_{45}N_{23}V$, M_5VV, and M_4VV transitions, respectively. Typical contaminations like carbon 1s and oxygen 1s are expected at kinetic energies of $E_{kin} = 350\,\mathrm{eV}$, and $E_{kin} = 110\,\mathrm{eV}$, respectively.
For a more in-depth analysis a high resolution XPS spectrum of the Ag 3d signal was recorded. The incoming photon energy was $h\nu = 480\,eV$ and the spectrum was measured in normal emission mode. For background substraction the Tougaard-background was applied to

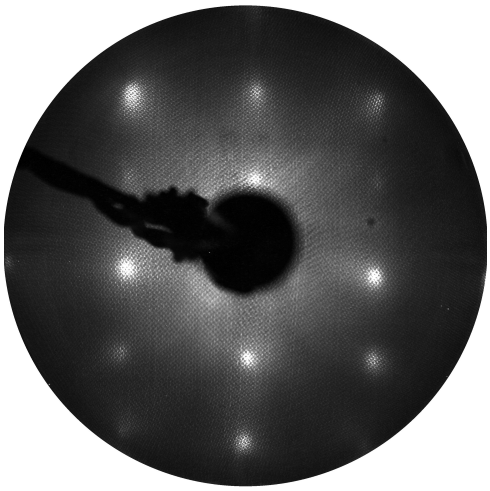

Figure 1: LEED pattern of the (1x1)-reconstructed Ag(110) surface. The energy of the incoming electrons is $E_{kin} = 120\,\mathrm{eV}$.

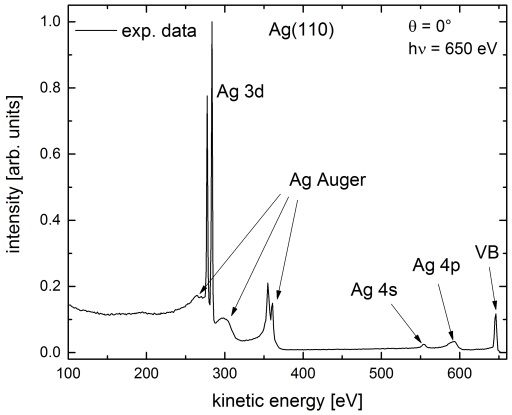

Figure 2: XPS spectrum of the clean Ag(110) substrate after several cycles of annealing and sputtering. Ag 3d, 4s, and 4p core-levels are well resolved. Also, the Ag MNN Auger lines are visible. No indication for oxygen or carbon contamination is visible.

the spectrum [14]. For analysis of the high-resolution spectrum a fitting procedure was performed. The peak shape $f(E)$ can be described by a convolution of Gaussian function G and a Doniach-Sunjic function D

$$f(E) = \sum_i A_i \cdot (G(\sigma_{g,i}) * D(\sigma_{ds,i}, \alpha_i, E_i))\,(E) \quad (1)$$
$$+A_i \cdot h_{SO} \cdot (G(\sigma_{g,i}) * D(\sigma_{ds,i}, \alpha_i, E_i - \Delta E_{SO}))\,(E),$$

where A_i denotes the amplitude, $\sigma_{g,i}$ the Gaussian full width at half maximum (FWHM), $\sigma_{ds,i}$ the FWHM of the Doniach-Sunjic profile, and α_i the asymmetry parameters [15]. E_i is related to the kinetic energy of the component. Component splitting due to spin-orbit-coupling (SO) was taken into account by the parameters h_{SO} and ΔE_{SO}. The XPS spectrum of the Ag 3d signal was fitted to one spin-orbit splitted component as shown in figure 3. Furthermore, three dominant plasmon excitations are clearly visible in the XPS spectrum. These plasmon excitations are E_{P1}, E_{P2}, and E_{P3} and they are shifted by 4 eV, 8 eV, and 10 eV with respect to the Ag $3d_{5/2}$ component, respectively.
From these in-depth analysis of LEED pattern and XPS spectra we can conclude that we have a well-ordered and well-reconstructed clean Ag(110) surface for the growth of silicene nano-ribbons.

3 RESULTS

For deposition of (5×2)-reconstructed silicene nano-ribbons on the Ag(110) surface the bare substrate was heated to $T = 230\,^{\circ}\mathrm{C}$ during deposition. The deposition of silicon was performed by a direct current evaporator with a distance of approximately 25 cm to the substrate. The time of evaporation was 120 min.
The successful deposition of silicon on Ag(110) forming silicene nano-ribbons was confirmed by analyzing a high resolution XPS spectrum of the Si 2p signal. This spectrum is shown in figure 4. The Si 2p spectrum was recorded at in incoming photon energy of $h\nu = 180\,\mathrm{eV}$ in normal emission mode. The Si 2p signal is split into two components due to spin-orbit coupling. The spin-orbit coupled components are shifted by 0.6 eV. This is in agreement with literature [17]. Additionally each spin-orbit component consists of two chemical shifted components. These components are shifted by approximately 0.2 eV. Also, it is obvious that the peak has an asymmetric shape. The peak shape and the relative locations of the chemical shifted components are in great agreement with values reported in previous works [16]. From the existence of two chemically shifted components it can be concluded that the unit cell of silicene consists of silicon atoms with two different chemical environments. This has to be taken into account when proposing structure models of silicene.

A high resolution XPS spectrum of the Ag 3d signal after successful growth of silicene nano-ribbons is displayed in figure 5. The spectrum is recorded at an incoming photon energy of $h\nu = 450\,\mathrm{eV}$ in normal emission mode. In comparison to figure 3 the three plasmon excitation peaks vanished. This XPS spectrum was fitted with one spin-orbit component as the XPS spectrum before silicon deposition. The fitting parameters are nearly the same, and the line-shape remains unchanged. From comparing the XPS spectra before and after silicon deposition as shown in figure 3 and 5 we conclude on two different binding scenarios at the surface. First, conservation of the line-shape indicates that no new chemical bond was established due to sil-

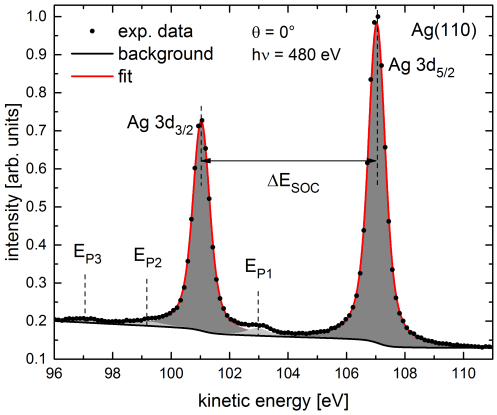

Figure 3: High-resolution XPS spectrum of the clean Ag(110) after successful preparation. Spin-orbit splitting of the Ag 3d core-level is clearly visible. Also, the three dominant plasmon excitations are referenced as E_{P1}, E_{P2}, and E_{P3}.

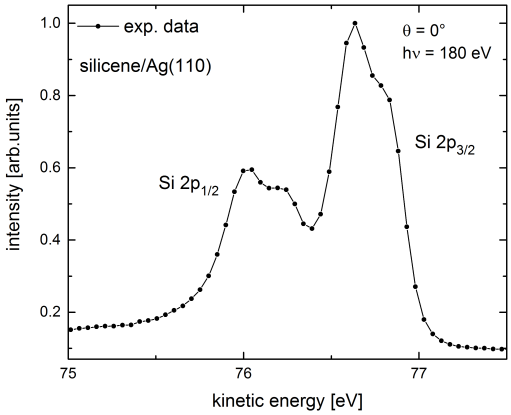

Figure 4: High-resolution XPS spectrum of the Si 2p signal after evaporation of silicon on the prepared Ag(110) substrate. An asymmetric lineshape of the Si 2p signal is clearly visible. Also, the characteristic double peak structure of silicene is shown.

icon adsorption. Thus, this is a hint for a weak van-der-Waals bond between the Ag(110) substrate and the silicene nano-ribbons. Another scenario could be that only a bonding type with no or an unresolved chemical shift is present at the surface.

4 CONCLUSION

In conclusion, we report on the preparation of (1×1)-reconstructed Ag(110) and (5×2)-reconstructed silicene nano-ribbons on Ag(110). Evidence of successful preparation is given by LEED measurements as well as XPS spectra. The analysis of the Si 2p signal reveals that silicene nano-ribbons on Ag(110) inhibit silicon atoms in two different chemical environments. From the analysis of the Ag 3d signal no conclusive confinement could be deduced for validating different structure models. The most recent proposed structure of silicene nano-ribbons on Ag(110) consists of a so-called pentamer structure. We will link our experimental results with the pentamer structure shown in figures 6 and 7. The pentamer structure can be described as a buckeld pentagonal structure consisting of 12 atoms in its unit cell. The silicon atoms are existent in two different chemical environments. This observation fits to our analysis of the Si 2p signal. The distance between the Ag(110) substrate and the adsorbed silicene nano-ribbons is small, thus a covalent bonding is likely. This fits to the second mentioned scenario indicating an unresolved chemical shift at the surface.

For a more sophisticated structure analysis we plan further photoelectron diffraction (XPD) experiments. Since XPD measurements are sensitive to the atom position of the individual emitting atoms we expect to conclude on the local structural environments of the emitting atoms. Since the phase information is lost during the measurement, the measured XPD pattern will be compared to simulated XPD pattern for the various proposed structure models [2-13]. By this procedure we will be able to determine the correct structure describing silicene nano-ribbons.

REFERENCES

[1] Davila et al., Nanotechnology 23, 385703, 2012.
[2] G.-m. He, Phys. Rev. B 73, 035311, 2006.
[3] C. Leandri, Ph.D. thesis, Marseille, 2004.
[4] B. Aufray et al., Appl. Phys. Lett. 96, 183102, 2010.
[5] H. Sahaf et al., Appl. Phys. Lett. 90, 263110, 2007.
[6] C. Hogan et al., Phys. Rev. B 92, 115439, 2015.
[7] J.I. Cerda et al., Nat. Commun. 7, 13076, 2016.
[8] R. Bernard et al., Phys. Rev. B 88, 121411, 2013.
[9] P. Lagarde et al., J. Phys.: Condens. Matter 28, 075002, 2016.
[10] C. Lian et al., Phys. B Condens. Matter 407, 4695, 2012.
[11] H. Sahaf et al., EPL 86, 28006, 2009.
[12] B. Feng et al., Surf. Sci. 645, 74, 2016.
[13] G. Prevot et al., Phys. Rev. Lett. 118, 049901, 2017.
[14] S. Tougaard, Surf. Interface Anal. 11, 453, 1988.
[15] S. Doniach et al., J. Phys. C 3, 285, 1970.
[16] P. De Padova et al., Nano Lett. 8, 271, 2008.
[17] E. Landemark et al., Surf. Sci. 287, 529, 1993.

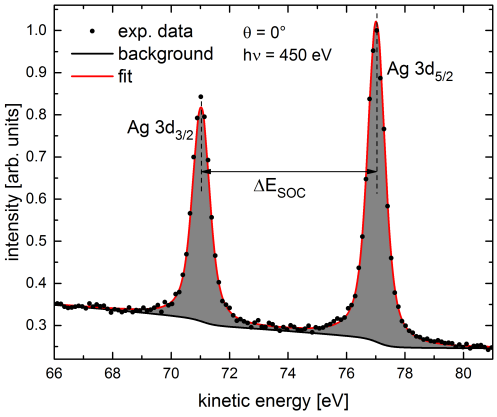

Figure 5: High-resolution XPS spectrum of the Ag(110) after evaporation of silicon. The plasmon excitation peaks vanished in comparison to figure 3. The shape of the Ag 3d core-level signal remains unchanged.

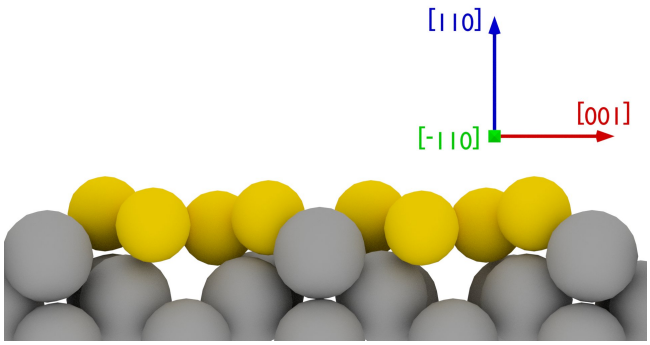

Figure 6: Side-view of the latest proposed structure model by Prevot et al. [13].

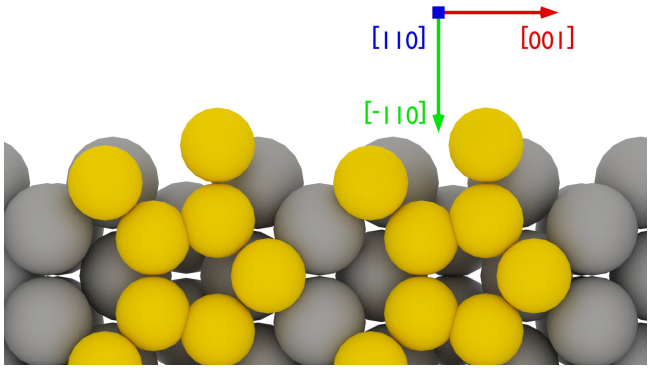

Figure 7: Top-view of the latest proposed structure model by Prevot et al. [13].

TechConnect Briefs 2017, TechConnect.org, ISBN 978-0-9975117-8-9